

Growth of ZnO films on Si(111) by metalorganic chemical vapor deposition with AlN and low-temperature ZnO double buffers

Changda Zheng^{1,a}, Li Wang¹, Wenqing Fang¹, Fengyi Jiang¹

¹National Engineering Technology Research Center for LED on Si Substrate, Nanchang University, 330047, China

^azhengchangda@ncu.edu.cn,

Keywords: ZnO thin films; Chemical vapour deposition; ZnO buffer; AlN buffer; Si(111) substrate

Abstract. To enhance the quality of ZnO films on Si(111) substrate, single layers of low-temperature ZnO (LT-ZnO) and AlN, as well as a combination of AlN and LT-ZnO layer, were used as intermediate layers by atmospheric pressure metalorganic chemical vapor deposition system. Only polycrystalline ZnO film was formed when a LT-ZnO single buffer was used. Crystal quality was enhanced when LT-ZnO was replaced by 20 nm AlN as the single buffer. The full width at half maximum (FWHM) of ZnO(0002) x-ray diffraction ω -rocking curve was 642 arcsec. Cracks began to appear on the film surface as crystallinity was enhanced. A ZnO mosaic single-crystal film with a mirror-like surface was successfully fabricated when a combined AlN and LT-ZnO served as buffer, and its FWHM of ZnO(0002) ω -rocking curve peak was only 460 arcsec. The film surface was smoother but cracks were still evident on the film. Contrary to the three-dimensional growth mode of samples with a single buffer, a quasi-two-dimensional growth mode was realized for the double-buffered high-temperature ZnO layer. Calculated film thickness was 2.14 μm , and the growth rate reached 4.3 $\mu\text{m}/\text{h}$ based on the laser in situ laser reflectance trace.

Introduction

Wide bandgap semiconductor materials such as gallium nitride (GaN) and zinc oxide (ZnO) have been extensively studied and applied in short-wavelength optical devices [1,2]. ZnO has some distinct advantages over competing materials because of its prominent material physical properties. This material has a bandgap of 3.37 eV at room temperature (RT) and large exciton binding energy of 60 meV, providing an attractive prospect to practical low-threshold excitonic laser diode [3]. To achieve high-performance ZnO photoelectronic devices, the fabrication of high-quality P-type ZnO material has become a principal challenge and the hottest research point [4]. However, the foremost important step and requirement is the production of high-quality intrinsic ZnO film with good crystallinity and low-density intrinsic carrier concentration. Sapphire has been widely used as the heteroepitaxy substrate for ZnO film growth [5,6]. However, several intrinsic physical characteristics of Al_2O_3 , such as high hardness, electrical insulation, and poor thermal conductivity, complicate and hinder prospective device fabrication processes and device applications. Thus, some researchers have begun to focus on the silicon (Si) substrate due to its good electrical and thermal conductivities, low cost, high crystal quality, and availability of large size single crystal [7]. Si has become an attractive candidate substrate for the ZnO epilayer.

Several difficulties are still encountered when a Si substrate is used. First is the oxidization of the Si substrate by an oxygen (O) source (such as H_2O , O_2 , CO_2 , etc.) during the initial growth step, which will result in poor-quality ZnO film on its surface. Second, the big mismatch (including lattice and thermal mismatches) between ZnO and Si will cause high density dislocation and low crystallization on the ZnO film. Therefore, several buffers such as AlN [8], Al_2O_3 [9], SiC [10], GaN [11], Y_2O_3 [12], $\gamma\text{-LiAlO}_2$ [13] and ZnS [14] have been employed to inhibit these difficulties in enhancing film quality.

In our previous work, high-quality ZnO/AlN/Silicon(111) film was successfully grown on Si(111) using an atmospheric pressure metalorganic chemical vapor deposition (AP-MOCVD) system [15]. In the present paper, we further studied the roles of the single AlN, single low temperature (LT)-ZnO, and a combination of AlN and LT-ZnO buffers on the properties of ZnO films grown on Si(111) substrates. The effects of various buffers on the surface topography morphology, crystallinity, and growth model of ZnO film were evaluated and discussed.

Experimental Details

ZnO films were grown on Si(111) substrates by AP-MOCVD. In situ interference monitoring is performed with a 635 nm laser. Diethylzinc and pure water (H₂O) were used as Zn and O sources, respectively. The Zn and O sources were transferred by pure nitrogen carrier gas and independently injected into a reactor before reaching into the reactor to restrain the pre-reaction between them. Si substrates were degreased by H₂SO₄:H₂O₂=3:1 mixture solution and etched with diluted HF solution to remove the surface oxide layer.

Three samples were prepared in the experiment. For sample A, ZnO film was directly grown on the Si(111) substrate by a two-step process: A homogeneous LT-ZnO buffer was initially grown at 300 °C for 1 min after annealing at 800 °C for 20 min, and then a high-temperature (HT)-ZnO epitaxy layer was grown at 680 °C for 30 min. For samples B and C, a 200 nm AlN layer was initially deposited on the Si(111) substrate by Thomas Swan low-pressure close-coupled showerhead reactor system. Al and N precursors were TMAI and NH₃, respectively. Afterward, the AlN/Si(111) templates were transferred to the AP-MOCVD system as substrate. For sample B, the HT-ZnO film was directly grown on the AlN/Si(111) template at 680 °C. For sample C, the same growth conditions were adopted as those of sample A, except that the AlN/Si(111) substrate was used instead of the Si(111) substrate. The detailed growth conditions are also listed in Table 1.

Table 1: Primary growth conditions for samples A, B, and C with various buffer layers.

| Sample | <i>LT-ZnO growth</i> | | <i>Recrystallization process</i> | | <i>HT-ZnO growth</i> | | |
|--------|----------------------|-------------|----------------------------------|--------------------|----------------------|--------------------|----|
| | <i>AlN</i> | | | | | | |
| | <i>T[°C]</i> | <i>t[s]</i> | <i>T[°C]</i> | <i>T [minutes]</i> | <i>T[°C]</i> | <i>T [minutes]</i> | |
| A | / | 300 | 60 | 800 | 20 | 680 | 30 |
| B | Yes | / | / | / | / | 680 | 30 |
| C | yes | 300 | 60 | 800 | 20 | 680 | 30 |

Crystal quality was investigated using a Bede D1 System X-ray Diffractometer System. Surface morphologies of the samples were examined using an Olympus-BX51 differential interference contrast microscope and a Benyuan CSPM-4100 atomic force microscope (AFM). Film growth was also monitored in situ by an interferometer with a 635 nm semiconductor laser.

Results and Discussion

The three samples (i.e., ZnO/LT-ZnO/Si, ZnO/AlN/Si, and ZnO/LT-ZnO/AlN/Si) were arrayed alongside. Only the double-buffered sample C presents a relatively smooth mirror-like surface. This structure is contrary to the coarse surfaces of the other two single-buffered samples, as verified by the differential interference microscope and illustrated in Fig. 1. The surface gradually becomes smoother and flatter from sample A to sample C. A frosted glass-like surface is manifested by sample A after visual check due to light scattering caused by the hackly surface.

However, some cracks are visible on the film surface images of samples B and C, which are conspicuously absent on sample A. The cracks are parallel to one another or intersect at either 60° or 120°. Considering the crack propagation and ZnO plane direction, the cracks are propagated along the

ZnO $\langle 11\text{-}20 \rangle$ directions. We infer that the cracks originated from the difference in the thermal expansion coefficient between the ZnO layer ($4.75 \times 10^{-6} \text{ K}^{-1}$) and the silicon substrate ($2.62 \times 10^{-6} \text{ K}^{-1}$) when the sample temperature cooled down from a high-growth temperature to RT.

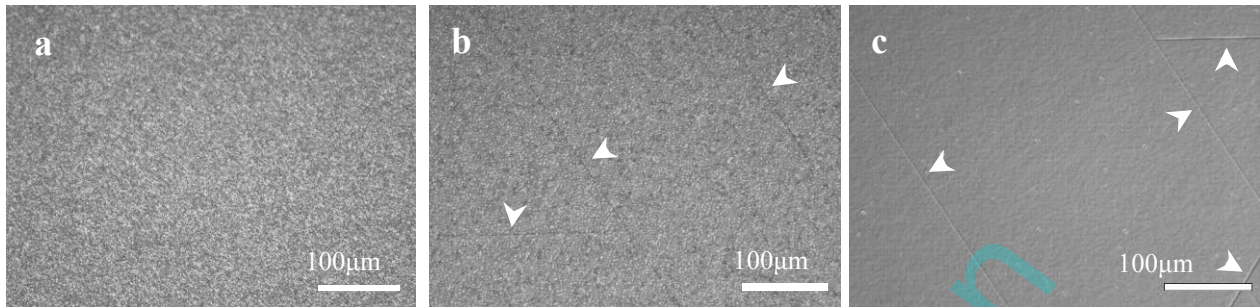


Fig. 1: Surface topography of the ZnO films by differential interference microscopy: a) with LT-ZnO single-buffer layer, b) with AlN single-buffer layer, and c) with AlN and LT-ZnO double buffer.

To characterize the film orientation and crystallinity of the samples, X-ray diffraction (XRD) θ - 2θ and ω -rocking scans were introduced. All the θ - 2θ scanning curves (not shown in the paper) exhibit a relatively high intensity peak due to the ZnO(0002) plane diffractions. This testifies that the three ZnO films have c-axis-preferred orientations. Fig. 2 displays the ω -rocking curves of ZnO(0002) planes of samples B and C.

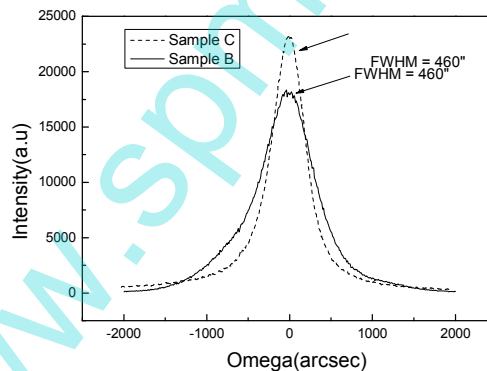


Fig. 2: Double crystal X-ray diffraction rocking curves of symmetrical ZnO(0002) planes of samples B and C.

No peak was observed in sample A when the XRD rocking curve test was applied due to its poor crystalline quality. The AlN buffer used in sample B resulted in a significantly enhanced crystal film. The FWHM of (0002) plan ω -rocking curve is only 642 arcsec. Thus, the ZnO film crystal orientation is significantly enhanced by the introduction of the AlN buffer. The role of AlN may be summarized as follows: First, AlN can be easily nucleated on the Si surface [16] and protects the substrate from being oxidized. Second, the thermal expansion coefficient of AlN ($4.20 \times 10^{-6} \text{ K}^{-1}$) is between those of ZnO and Si, which can also eliminate the thermal mismatch to a certain extent. Last, the lattice constant of AlN is less than that of ZnO, which would introduce compressive stress to the ZnO film. All these are advantageous in improving the qualities of ZnO on Si substrate. Furthermore, the FWHM value of sample C is decreased to only 460 arcsec. For this sample, HT-ZnO was buffered with 20nm LT-ZnO buffer layers on an AlN/Si template. Thus, the enhancement on the film quality is attributed to the LT-ZnO buffer. The LT-ZnO layer grown under 300 °C can be easily nucleated onto the AlN/Si template surface because of its large sticking coefficient and amorphism. The LT-ZnO

buffer layer can also reduce the stress between HT-ZnO layer and substrate from lattice and thermal mismatch. Point defects formed in the LT-ZnO would also interact with dislocation and improve the quality of top HT-ZnO epilayer [17-19].

Fig 3 shows the in situ laser interference growth curves. Variations in the interference line shape and swing among the three samples were observed during the HT-ZnO growth. Only five regular interference periods were observed for sample A. The amplitude is gradually reduced and almost reached zero at the fifth period. The inset AFM picture reveals that the film is discontinuous and consisted of randomly distributed ZnO islands, which is consistent with the laser interference results. For sample B, the interference line shape is similar to that of sample A but the number of regular interference periods increased from 5 to 7. AFM topography also becomes more continuous, and the film is composed of closely arrayed ZnO grains. For sample C, regular interference periods appear all along the HT-ZnO growth, which indicates that a quasi-two-dimensional growth mode has been realized. The surface also becomes continuous with corresponding pyramid topography. The calculated thickness of the ZnO film is 2.14 μm , and growth rate is 4.3 $\mu\text{m}/\text{h}$. The high growth rate is significantly beneficial for the future industrialization of the ZnO semiconductor film.

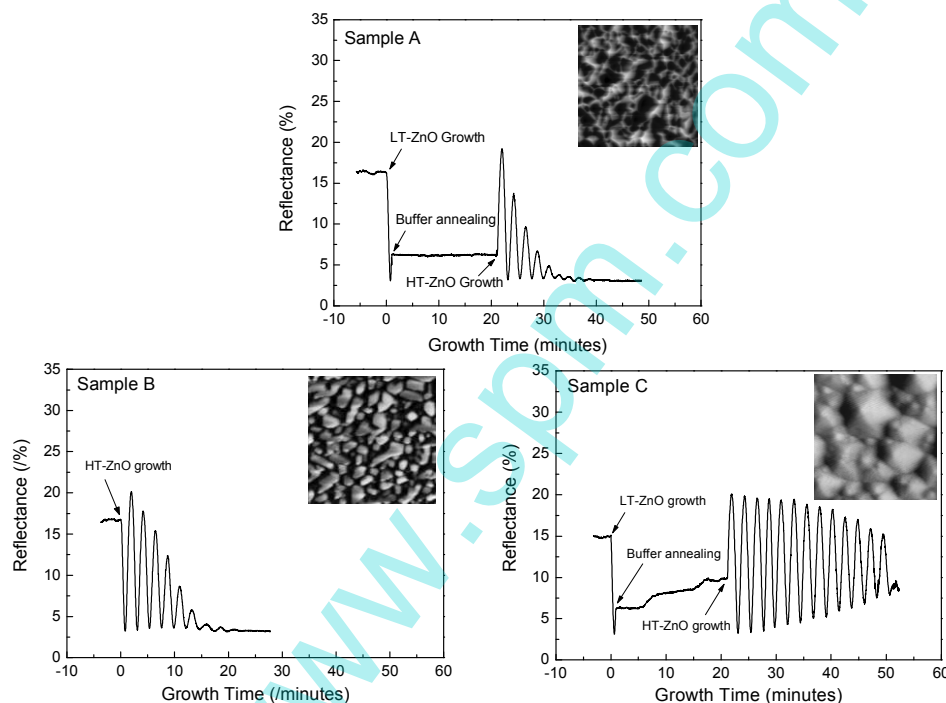


Fig. 3: In situ laser reflectance traces of ZnO film growth for the three samples. The inset graphs are the corresponding $5 \times 5 \mu\text{m}^2$ AFM topographies.

Summery

In conclusion, the properties of the ZnO film on a Si(111) substrate are significantly enhanced by the introduction of AlN and LT-ZnO double-buffer layers. A mirror-like surface ZnO film is successfully obtained. However, some cracking lines are still evident on the 2.14 μm layer, which is accompanied by the crystal improvement and great stress from thermal mismatch. Quasi-two-dimensional growth mode is achieved when the growth rate reaches 4.3 $\mu\text{m}/\text{h}$. AlN layer initially protects the silicon surface from oxidation and the first stress relax layer. The LT-ZnO buffer layer further reduces the stress between the HT-ZnO layer and substrate, thereby improving the quality of the HT-ZnO epilayer. The successful growth of high-quality ZnO single layer materials on a Si substrate establishes a good foundation for the future growth of ZnO optoelectronic device materials.

Acknowledgements

This work was financially supported by Science and Technology Staff Service Enterprise Project of the Ministry of Science and Technology of China (No. 2009GJC50021)

References:

- [1] D C Look, B Claflin, Y I Alivov and S J Park: *Phys Status Solidi a* Vol. 201 (2004), p. 2203
- [2] C Klingshirn, J Fallert, H Zhou, J Sartor, C Thiele, F Maier-Flaig, D Schneider and H Kalt: *physica status solidi (b)* Vol. 247 (2010), p. 1424
- [3] Z K Tang, G K L Wong, P Yu, M Kawasaki, A Ohtomo, H Koinuma and Y Segawa: *Appl Phys Lett* Vol. 72 (1998), p. 3270
- [4] D C Look: *Mat Sci Eng B-Solid* Vol. 80 (2001), p. 383
- [5] K Postava, H Sueki, M Aoyama, T Yamaguchi, C Ino, Y Igasaki and M Horie: *J Appl Phys* Vol. 87 (2000), p. 7820
- [6] J H Park, C B Lee, I S Kim, S J Jang and B T Lee: *Thin Solid Films* Vol. 517 (2009), p. 4432
- [7] X Feng, J Kang, W Inami, X Yuan, M Terauchi, T Sekiguchi, S Tsunekawa, S Ito and T Sakurai: *Cryst Growth Des* Vol. 7 (2007), p. 564
- [8] C Jin, R Narayan, A Tiwari, H Zhou, A Kvit and J Narayan: *Materials Science and Engineering B* Vol. 117 (2005), p. 348
- [9] M Kumar, R M Mehra, A Wakahara, M Ishida and A Yoshida: *J Appl Phys* Vol. 93 (2003), p. 3837
- [10] J J Zhu, B X Lin, X K Sun, R Yao, C S Shi and Z X Fu: *Thin Solid Films* Vol. 478 (2005), p. 218
- [11] A Nahhas, H K Kim and J Blachere: *Appl Phys Lett* Vol. 78 (2001), p. 1511
- [12] W R Liu, Y H Li, W F Hsieh, C H Hsu, W C Lee, Y J Lee, M Hong and J Kwo: *Cryst Growth Des* Vol. 9 (2009), p. 239
- [13] J Zou, S Zhou, J Xu, X Zhang, X Li, Z Xie, P Han and R Zhang: *J Mater Sci* Vol. 41 (2006), p. 5937
- [14] T Onuma, S F Chichibu, A Uedono, Y Z Yoo, T Chikyow, T Sota, M Kawasaki and H Koinuma: *Appl Phys Lett* Vol. 85 (2004), p. 5586
- [15] F Jiang, C Zheng, L Wang, W Fang, Y Pu and J Dai: *J Lumin* Vol. 122-123 (2007), p. 905
- [16] A Watanabe, T Takeuchi, K Hirose, H Amano, K Hiramatsu and I Akasaki: *J Cryst Growth* Vol. 128 (1993), p. 391
- [17] H S Kang, S S Pang, J W Kim, G H Kim, J H Kim, S Y Lee, Y Li, H Wang and Q X Jia: *Superlattice Microst* Vol. 40 (2006), p. 501
- [18] F Xiu, Z Yang, D Zhao, J Liu, K A Alim, A A Balandin, M E Itkis and R C Haddon: *J Cryst Growth* Vol. 286 (2006), p. 61
- [19] J F Yan, Y M Lu, Y C Liu, H W Liang, B H Li, D Z Shen, J Y Zhang and X W Fan: *J Cryst Growth* Vol. 266 (2004), p. 505